Paradigm Academic Press
Innovation in Science and Technology
ISSN 2788-7030
JAN. 2025 VOL.4, NO.1

Review of the Processing Parameters of the Plasma Electrolytic Oxidation on Titanium Alloys for Biological Application

Mengmeng Tian[1], Yijia Guan[1], Feihu Zhao[1], Youfu Xiong[1], Jiaqi Bai[1], Wanyu Zhao[1], Xiaofeng Jia[1], Hui Guo[1] & Hongshan San[1]

[1] School of Materials Science and Engineering, Henan Polytechnic University, Jiaozuo 454000, China

Correspondence: Hongshan San, School of Materials Science and Engineering, Henan Polytechnic University, Jiaozuo 454000, China.

doi:10.56397/IST.2025.01.01

Abstract

Recently, calcium phosphate (Ca-P) based composites, such as hydroxyapatite (HA) and carbonate apatite (CA), have gained attention as desirable bioactive coatings. These coatings have the power to improve implant materials' biocompatibility and speed up the process of osseointegration between the implant and host bone. Moreover, bioactive layers are formed when titanium implants oxidize in solutions containing calcium and phosphorus compounds, which greatly shortens the time needed for implant osseointegration. Furthermore, the characteristics of PEO coatings on titanium and titanium alloys are largely dependent on the electrolyte's composition, additives, temperature, and electrical factors. This paper focuses on how PEO coating of pure titanium and other biomedical-grade titanium alloys is affected by electrolyte's composition, additives, temperature, and electrical parameters (power source, frequency, voltage, oxidation duration, and current density). Importantly, these traits can alter the ultimate form, composition, and crystal structure of the coating. This review emphasizes the significance of the PEO procedure, current advancements, and potential areas for further research. By gaining a more profound comprehension of the components of bioactive coatings, scientists can enhance their efficiency in orthopedic and dental implants, thus streamlining the production process.

Keywords: calcium phosphate, biocompatibility, osseointegration, plasma electrolytic oxidation, titanium alloys, implants

1. Introduction

Micro-arc oxidation (MAO), often known as plasma electrolytic oxidation (PEO), is a novel technique for coating metals with thick, intricate, and dense oxide-ceramic coatings that may improve wear, corrosion resistance (S. Sikdar et al., 2021) and biocompatibility. As is well known, PEO is a widely used technique for creating surface-modified oxide coatings on light metals, which particularly for creating porous oxidation layers on pure titanium and titanium alloys (A. Fattah-alhosseini et al., 2020). During the process of PEO, multiple pores and rough texture structure and nano-scale surface topography are formed (S. Abbasi et al., 2007). Topographical layers of surfaces with a less than 100 nm roughness are extensively used across multiple sectors, such as the mechanical, petrochemical, and biomedical (H. Shi et al., 2021), due to it proven efficacy in improving osteoblast cell adhesion and growth (W.-H. Song et al., 2004). PEO has proven to be a viable method for enhancing the biocompatibility of metal implants due to ongoing research into its mechanism. It has been shown to have a high degree of cytocompatibility and initial adhesion, as well as an innate capacity to encourage MSC osteo-differentiation, indicating significant potential for bone repair applications (P.B. Santos et al., 2021). Furthermore, the intricate structure and development of oxides in metal implants might impact their corrosion, wear, and biocompatibility characteristics. Incorporating bioactive components into the oxide layer shows potential for producing implant materials with superior chemical stability and osteointegration ability (P.B.

Santos et al., 2021; M. Kaseem & H.-C. Choe, 2021). Recently, calcium and phosphorus (Ca-P)-based composites have attracted much attention from the scientific and biomedical communities due to their unique biological and skeleton-like mechanical properties (J. Hadzik et al., 2023; M. Qadir et al., 2017). Additionally, PEO has proven effective in crafting Ca-Pcoating with nanoscale topographical features, fostering cell growth and eliciting specific reactions from adjacent tissues (R. Luo et al., 2013). This paper aims to discuss the PEO processing parameters used for preparing bioactive coatings on titanium from the four perspectives: electrolyte's composition, electrolyte's additive, electrolyte's temperature, and electrical parameters. It is important to adjust the coating process parameters to achieve these optimal performances.

2. Components of Electrolyte

In recent years, PEO technology has significantly advanced as a way to produce strong, wear-resistant, corrosion-resistant, and biocompatible coatings. Conducted usually within an aqueous solution electrolyte, the concentration and makeup of electrolytes in the PEO method play a crucial role in peak efficiency, influencing both the spark generation and component incorporation in the coating. Constituents within the electrolyte tend to accumulate on the surface of the specimen, impacting the processes at play and consequently influencing the type of substrate oxidation. Consequently, this affects the thickness, porousness, pore dimensions, and overall biocompatibility of oxide layers (A. Fattah-alhosseini et al., 2020). Via the PEO process, substances in the electrolytes can also be added to the coating. Given that carbonated apatite (Ca_5 (PO_4, CO_3)$_3$ (OH)) constitutes most bone tissues, preference arises for oxide coatings rich in calcium and phosphorus elements. These coatings exhibit favorable biological activity, evidenced by their capacity to induce HA precipitation in both in vitro and in vivo experiments (M. Sowa et al., 2013; A.R. Rafieerad et al., 2015; B.S. Necula et al., 2011). Applying HA to treated areas enables titanium alloys, processed via the PEO method, to maintain favorable mechanical characteristics. This attribute makes them exceptionally appropriate for orthopedic and dental implants, which enhances their osseointegration with human bones (A. Schwartz et al., 2022).

2.1 The Using of Electrolyte Composition

Inorganic (chloride (R. Zhou et al., 2014a), nitrate (K. Rokosz et al., 2017), phosphate (R. Zhou et al., 2014b), dihydrogen phosphates (A. Lugovskoy & S. Lugovskoy, 2014; Y. Bai et al., 2011)) or organic (acetate (C.A. Antônio et al., 2017; K.R. Shin et al., 2014) and β-glycerophosphate (A. Lugovskoy & S. Lugovskoy, 2014; A. Kossenko et al., 2013; S. Durdu et al., 2013; M.-A. Faghihi-Sani et al., 2013) calcium formate and calcium lactate solutions (J. Michalska et al., 2019)) calcium salts are introduced into electrolyte as calcium source. Phosphorus sources include phosphoric acid (H.-Y. Wang et al., 2014), phosphates (M. Aliofkhazraei et al., 2016; H. Sharifi et al., 2016; C.J. Chung et al., 2013), dihydrogen phosphates (W. Zhu et al., 2013; H.-T. Chen, et al., 2010; J.-z. Chen et al., 2006; M. Montazeri et al., 2011; S. Liu et al., 2011), sodium hexametaphosphate (J.-H. Ni et al., 2008) and β-glycerol phosphate disodium salt pentahydrate (β-GP) (S. Abbasi et al., 2012; M.-S. Kim et al., 2007; M.-A. Faghihi-Sani et al., 2013; S. Abbasi et al., 2013; D.-Y. Kim et al., 2009). Whether used separately or together, the electrolytic components result in vastly distinct coat structure and composition.

2.1.1 Inorganic

Some researchers investigated independently P-containing electrolytes. Zhang (2018) et al. studied porous TiO_2 coatings fabricated by PEO with a NaH_2PO_4 electrolyte. The coating containing P element shows an enhance of the osteoblast adhesion. Shin (2011) et al. applied two P-containing electrolytes, A: 0.02 M K_3PO_4 and B: 0.02 M $K_4P_2O_7$, under a current density of 200 mA/cm^2 for 300s. The coating prepared in $K_4P_2O_7$ electrolyte featured rougher surface as well as higher amount of anatase phase, leading to the excellent formation of the biomimetic apatite in the SBF solution. Moreover, many other elements have been used to modified the oxide coatings, such as fluoride (K. Venkateswarlu et al., 2013; V. K et al., 2013) and silicate (D. Krupa et al., 2012; L. Wang et al., 2014). Previous studies have demonstrated that fluoride-modified coating promote the development of fluoridated hydroxyapatite, which contributes to bone response and surface adhesion (J. Liang et al., 2005). Sodium silicate (Na_2SiO_3) was wildly used to enhance the wear resistance (J.R. Henstock et al., 2015; A. Kazek-Kęsik et al., 2014) and bioactivity of the PEO coating. This process can diminish the sparking voltage, hasten the coating's development, and alter its shape (J. Chen et al., 2024; D. Quintero et al., 2015) (in terms of pore dimensions and texture), thereby enhancing biocompatibility for the attachment and proliferation of rBMSCs (S. Wang et al., 2014; W. Simka et al., 2013).

Zhou (2014) et al. used CA (0.0375 mol/L) and Na_2SiO_3 (0.0465 mol/L) to prepare a bioactive coating. They achieved a coating with regular micropore shape and distribution (at a voltage range of 350~500V), and contains Ca, Si, Na, Ti and O elements (Figure 1). The composition of the PEO layers significantly influences the adhesion, proliferation, and ALP function of MC3T3-E1 cells (R. Zhou et al., 2014d). Furthermore, the coating effectively induces the varied nucleation and growth of apatite within simulated body fluid (SBF) (R. Zhou et al., 2014a). The implantation of this into a rabbit tibia reveals a unique amorphous configuration, enhanced by Si, Na, and Ca components, leading to a mechanical lock mechanism connecting the newly formed bones and the implants (R. Zhou et al., 2014e). Another electrolyte, comprising $Ca(CH_3COO)_2 \cdot H_2O$ (8.8 g/L), Na_2SiO_3 (7.1 g/L) and $Ca(H_2PO_4)_2 \cdot H_2O$ (6.3 g/L) to obtain a PEO coating containing Ca, P, Si and Na (R. Zhou et al., 2015a; R. Zhou et al., 2015b). San (2017) et al. used an electrolyte contains 11 g/L $Na_2SiO_3 \cdot 9H_2O$, 10 g/L $(NaPO_3)_6$ and 4 g/L $NaAlO_2$ in the PEO procedure. A continuous DC pulse voltage of 450 V, used for durations of 2 minutes and 20 seconds (with the voltage increment set at 5 V/s until hitting 450V), was implemented following an 8% duty cycle. For the Ti-6Al-4V substrate, the PEO coating also contains Al, V, Si and P, while Si and P originate from the electrolyte in the course of PEO processing. Observations reveal that the PEO coating contains Al, though the content is lower than the Ti-6Al-4V substrate, it should be avoided on the surface of a bone implant. On average, the thickness of the PEO coating is about 4.2 ± 0.2 μm (Figure 2). The immersion experiment indicates that the coating has the ability to induce HA deposit on it (Figure 3).

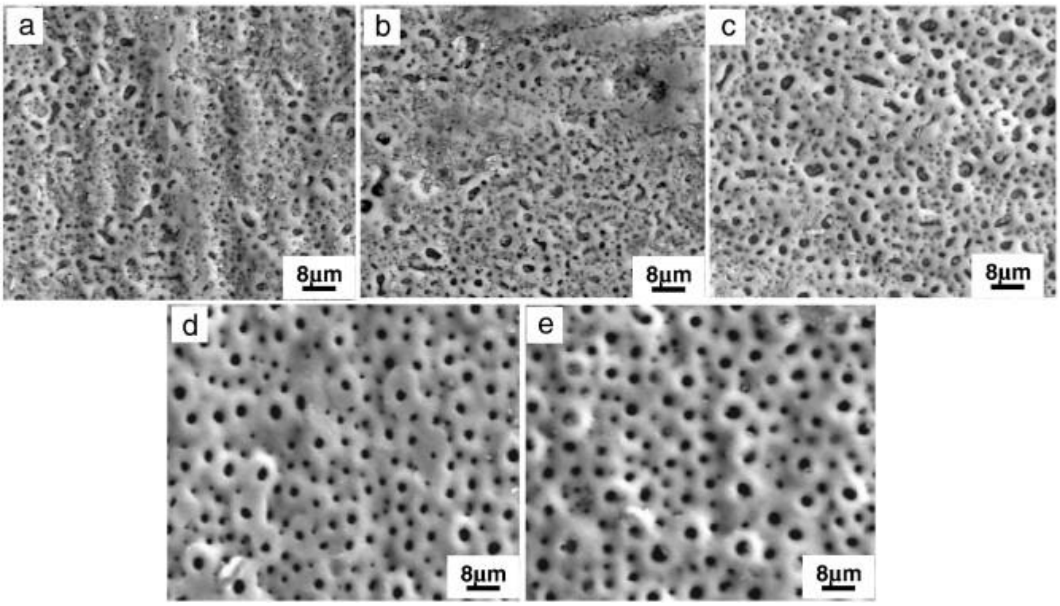

Figure 1. The typical SEM surface morphology of the APTN coatings formed at different applied voltages: (a) APTN200, (b) APTN250, (c) APTN300, (d) APTN350 and (e) APTN400 (R. Zhou et al., 2014c)

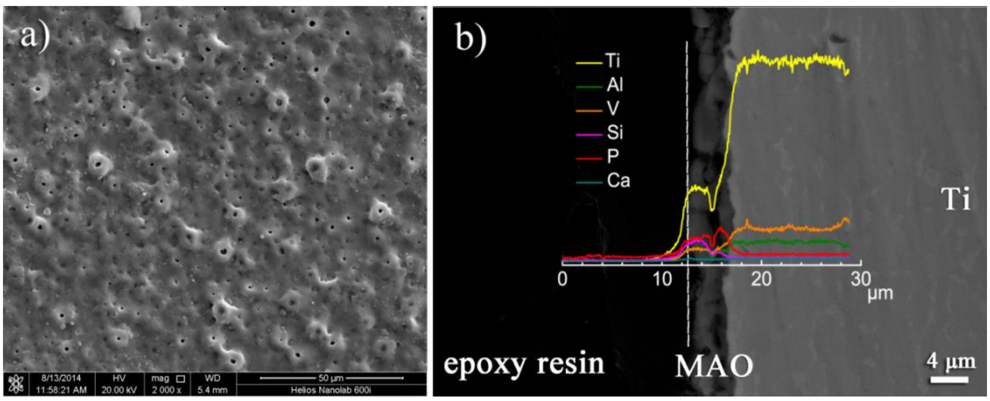

Figure 2. Surface (a) and cross-sectional (b) images of the PEO coatings (Hongshan San et al., 2017)

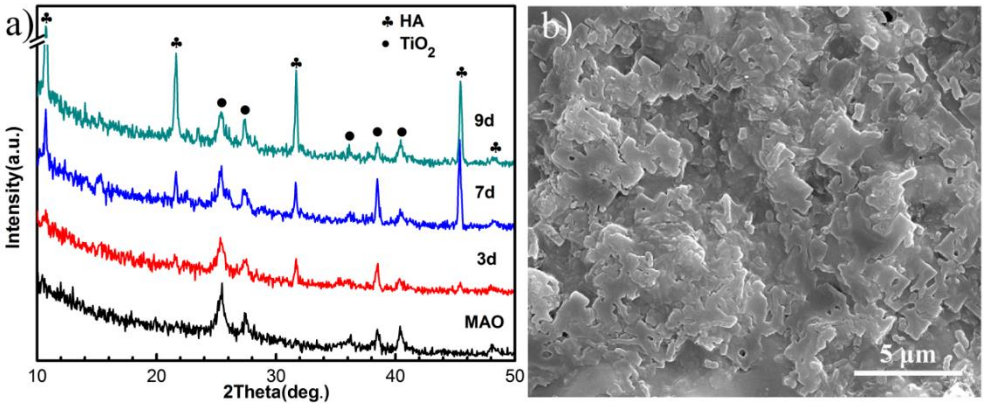

Figure 3. XRD patterns of the micro-arc oxidized Ti-6Al-4V sample immersed in SBF solution for the different times and the micrograph of the sample after 9 days of immersion: (a) XRD patterns of PEO substrate in SBF, (b) micrograph of the PEO substrate after 9 days of immersion (Hongshan San et al., 2017)

2.1.2 Organic

Kim (2009) et al. used 15 g·L-1 $C_3H_7Na_2O_6P\cdot5H_2O$ (β-GP) in the electrolyte form and incorporated an ethanol concentration of 0 to 50 vol.% to alter the PEO method. Without the addition of ethanol, a highly porous layer, presumably a TiO_2 phase, was observed on the specimen. With increased ethanol concentration, some of the pores were clogged. However, additional small pores appeared on the coating layer when a higher ethanol concentration (50 vol.%) was used. The formation of a HA/TiO_2 layer containing α-TCP and $CaCO_3$ on a Ti-6Al-4V alloy was investigated in an electrolyte containing 0.2 M CA and 0.02 M β-GP using different voltages (400 V, 430 V, 450 V, and 480 V) for 20 min via PEO. Observations showed a gradual decrease in the count of surface pores as the treatment duration extended from 1.5 minutes to 20 minutes (J. Sun, Y. Han & X. Huang, 2007). Over time, the pores vanished entirely following a 20-minute treatment.

In numerous researches, β-GP has been substituted with β-calcium glycerophosphate ($C_3H_7CaO_6P$, Ca-GP). Faghihi-Sani (2013) et al. engineered a HA layer on a Ti-6Al-4V alloy, employing 0.040 mol/L of Ca-GP and 0.232 mol/L of CA at a 100 Hz frequency, sustained for 4 minutes through PEO. The molar ratio of Ca/P in the HA layer is recorded as 1.67, with a thickness of 2.3 mm. Durdu (2013) et al. studied the production of HA on Ti-6Al-4V, employing CA and Ca-GP for varying electrolyte durations (1, 5, 10, 20, 40, 60, and 120 min). After 5 min, crystalline HA and calcium apatite-based phases as minor phases were formed in the coating structure and then the crystallinity of these phases increases with increasing treatment time. Variations in the quantity and dimensions of pores in the HA layer could fluctuate based on the length of time PEO is applied (Figure 4). Reports also indicate that sodium phosphate monobasic dehydrate ($NaH_2PO_4\cdot2H_2O$) and calcium six phosphate ($(NaPO_3)_6$) serve as substances for β-GP.

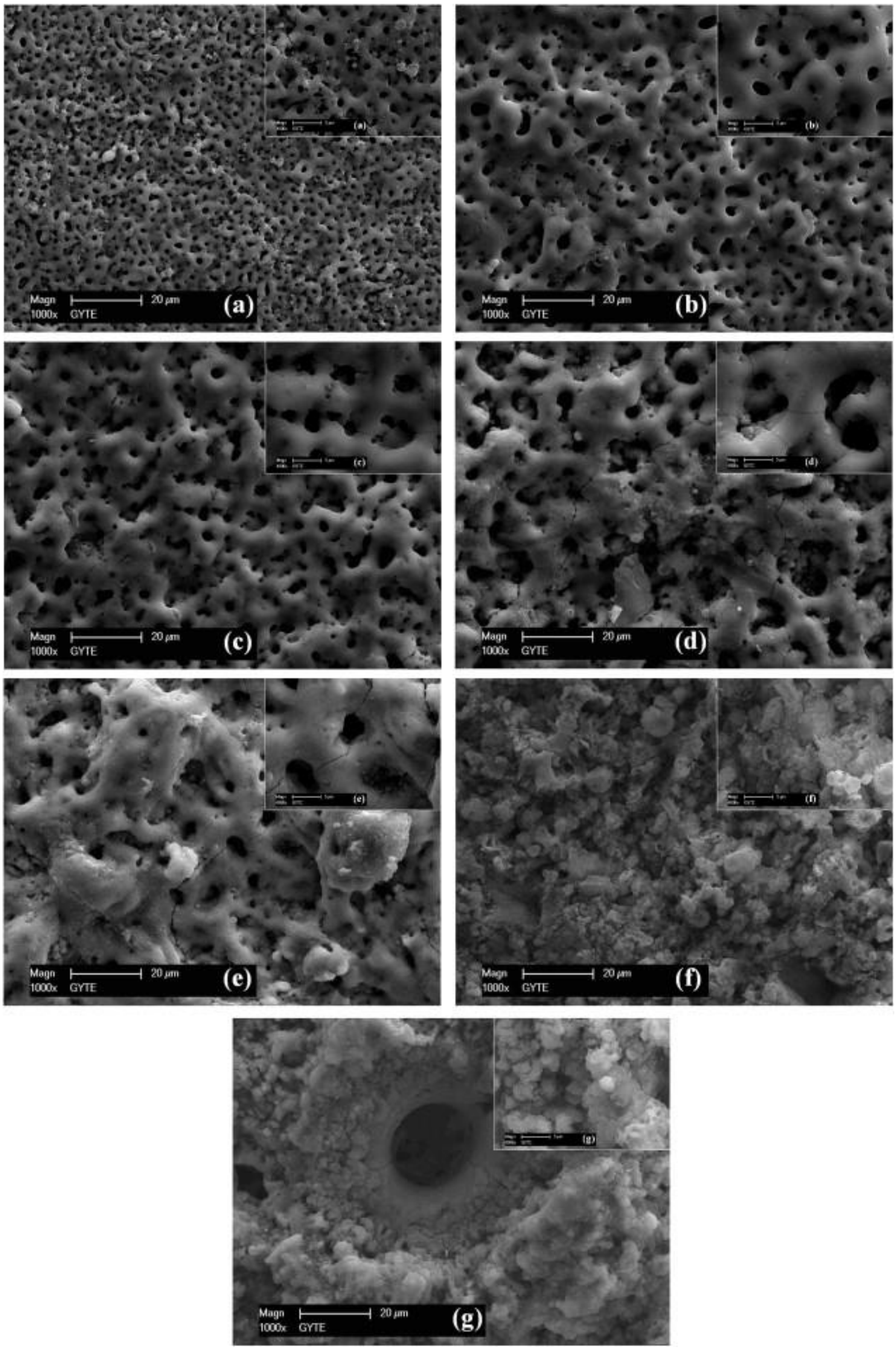

Figure 4. Surface morphologies of PEO coatings: (a) 1 min, (b) 5 min, (c) 10 min, (d) 20 min, (e) 40 min, (f) 60 min and (g) 120 min (S. Durdu et al., 2013)

2.2 The Influence of Electrolyte Concentration

Ni (2008) et al. used electrolytes with different concentrations of $NaH_2PO_4 \cdot 2H_2O$ and CA to obtain HA-containing coatings. Their study reported that the increase in the electrolyte concentration led to the reduction of the pore size of the coatings (from 5μm to 2μm). Moreover, the research indicated that enhancing the electrolyte concentration resulted in superior thickness and mechanical characteristics of BG-coated Ti surfaces (N.A. Sukrey et al., 2021). This indicates that increasing electrolyte concentration leads to a more even and compact coating, thereby improving the mechanical robustness and longevity of the coated material. Furthermore, the study investigated the biological efficacy of BG-coated titanium surfaces through an analysis of the bonding, growth, and diversification of rat bone marrow stem cells (BMSC). Findings revealed that surfaces coated with BG displayed a notable improvement in cell adhesion, growth, and transformation over pure Titanium surfaces. This demonstrates the capabilities of BG-coated Ti surfaces in fostering bone repair and bone integration. Some research opted for calcium chloride ($CaCl_2$) in place of CA. Kim (2007) et al. created an HA film in an electrolyte, varying the levels of $CaCl_2$ and potassium phosphate monobasic (KH_2PO_4) by employing the PEO method. In another study by Abbasi (2013) et al, samples were coated in electrolytes containing 5, 10, and 15 g/L CA and 1, 3, and 5 g/L β-GP at an optimized voltage for 3 minutes. It was found that increasing the concentration of CA and β-GP in the electrolyte had a similar effect on the average size of pores in the TiO_2/HAP layers (Figure 5). Additionally, the pore density decreased with increasing β-GP concentration, but the same decrease in pore density did not occur with increasing CA concentration. The highest fraction of porosity was observed in layers fabricated in electrolytes containing 1 g/L β-GP and 10 g/L CA. The synthesized layers consisted of HAp, anatase, $CaTiO_3$, and α-TCP phases in different proportions, depending on the electrolyte concentration. Hu (2012) et al. used a PEO electrolyte containing 0.1 mol/L CA and 0.05 mol/L β-GP to obtain a coating containing Ca and P. Their research focused on the growth of a bioglass (BG) (45S5) incorporated oxide layer via the PEO process on pure titanium (Ti) surfaces. The study investigated the effect of electrolyte concentration on the thickness and mechanical properties of the BG-coated Ti surfaces. The results showed that the lowest electrolyte concentration resulted in large sparks, indicating a higher level of energy and reactivity during the PEO process. Increasing the concentration of $CaCl_2$, thereby creating a rough microstructure of the HA film on the implant's surface during PEO, enhancing the bonding between organic bones and implants. HA films exhibited heightened crystallinity as $CaCl_2$ concentration rose, and a high concentration of calcium can promote the rapid growth of HA crystals (F. Liu et al., 2005).

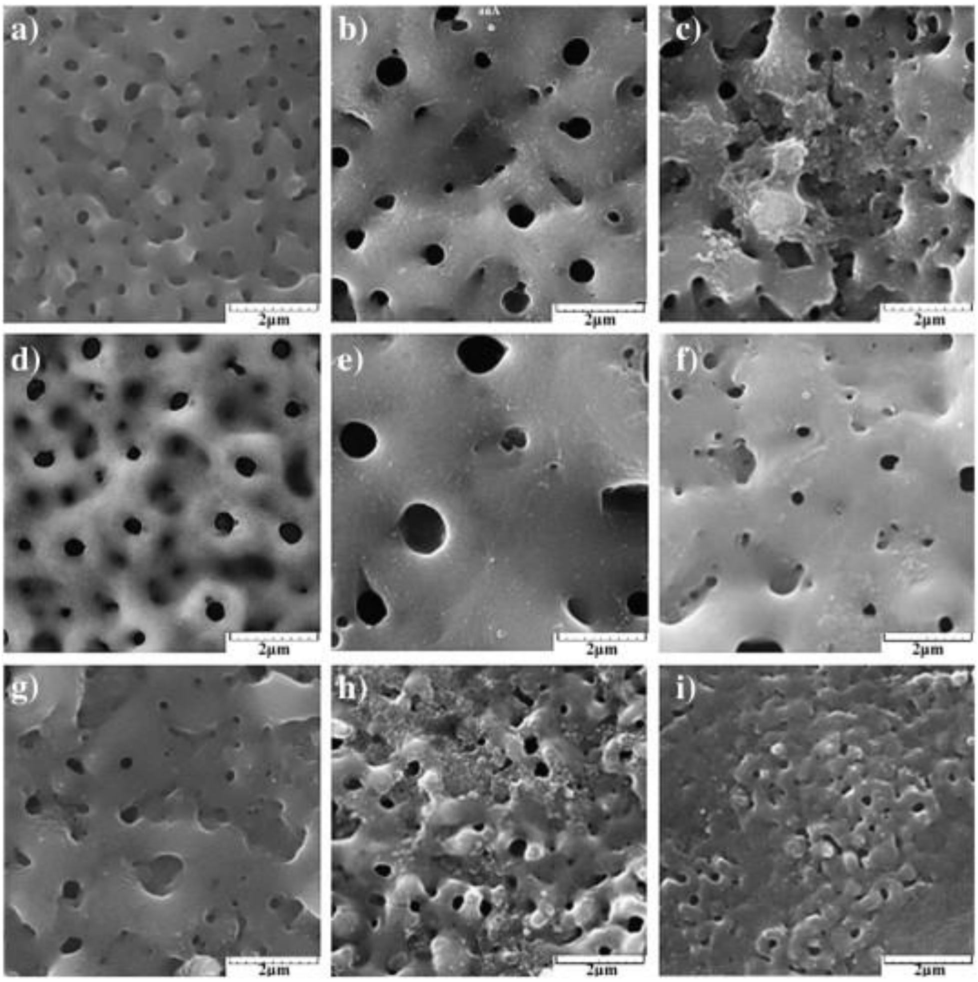

Figure 5. SEM images of the grown layers in electrolytes containing: a) 1, b) 3, c) 5 g/L β-GP and 5 g/L CA; d) 1, e) 3, f) 5 g/L β-GP and 10 g/L CA; g) 1, h) 3, i) 5 g/L β-GP and 15 g/L CA (S. Abbasi et al., 2013)

In conclusion, a huge range of electrolytes composed by the components above is in use. Among the many Ca element sources, CA was mostly used to introduce Ca element into the PEO coating. When calcium acetate is used as the calcium source, the arc discharge of the PEO process can be maintained at a small current density. The coating has a homogeneous porous morphology, and the calcium content of the coating is higher. More and finer calcium containing particles are gathered on the surface titanium and sintered into the coating under the local high temperature. Thus, a coating with higher calcium content can be obtained. However, there’s not any particular P element source that shows special advantages. Other components in the electrolyte containing F, Si, O or N element could benefit the PEO process and the biological properties of the coating. Some authors have improved the osseointegration and antibacterial activity of titanium alloys by preparing micro/nano-structured ceramic coatings doped with antibacterial element F through the PEO process on Ti6Al4V alloy in NaF electrolyte. In general, the coating formed in NaF electrolyte had low surface roughness and a great corrosion resistance, while increasing biocompatibility. Belkin et al. also found that anode plasma electrolytic saturation of titanium alloys with nitrogen and oxygen could decrease friction coefficient and increase wear resistance of the CP-Ti. This suggests that the appliance range of CP-Ti in our daily life could be increased (P.N. Belkin et al., 2016).

3. Electrolyte Additive

Extensive research has been conducted on PEO, focusing on its single-step method for enhancing the functionality of porous implant surfaces. Metallic nanoparticles, such as silver (Ag) (B.S. Necula et al., 2011; X. Zhang et al., 2018; N. Iqbal et al., 2014; S. Eraković et al., 2013; B.S. Necula wt al., 2012; B.S. Necula et al., 2009; I.A.J. van Hengel et al., 2017), copper (Cu) (X. Zhang et al., 2018; X. Yao et al., 2014; W. Zhu et al., 2013), zinc (Zn) (H. Hu et al., 2012; Y. Qiao et al., 2014; X. Shen et al., 2014) and their oxides have been employed most widely as antibacterial agents. Hengel (2021) et al. found that surfaces with Ag, Cu, Zn, or a mix of Ag, Cu, and Zn significantly decreased the bacterial count. The evaluation of PEO-exposed titanium implants infused with Ag, Cu, and Zn against implant-associated infections (IAI) necessitates the use of suitable bone infection models in vivo.

3.1 Addition of Metallic Nanoparticles

For instance, plasma electrolytic oxidation of pure titanium was performed using an Ag nanoparticles-loaded (A. Sobolev et al., 2019) calcium-phosphate solution with nitrilotriacetic acid (NTA). The resulting silver-enriched PEO layer exhibited effective antibacterial properties, high biocompatibility, and increased collagen production. Furthermore, ceramic coatings on titanium alloys have shown good antibacterial abilities and resistance to tribocorrosion, which are crucial for dental implants. That makes it a promising strategy for dental and orthopedic implant development (O. Oleshko et al., 2020). Besides, PEO was used to synthesize Cu_xO (CuO and Cu_2O) on the ceramic coating, enhancing its biological activity and tribocorrosion behavior (B. He et al., 2022). The addition of antibacterial elements like Ag, Cu, and Zn to the electrolyte enhances the PEO coating’s biological characteristics. To attain this, Kaseem (2021) et al. fabricated Ti-6Al-4V alloy implants in a stud screw shape using PEO. They used an electrolyte solution containing species such as Ag, Zn, Ca, P, etc. It was observed that the PEO treatment of dental implants resulted in the formation of more peripheral bone compared to sand-blasted implants.

3.2 Addition of GO

There is another new antimicrobial that has attracted a lot of attention recently. Graphene oxide (GO), a highly oxidized form of graphene, possesses excellent mechanical, antibacterial properties (W. Hu et al., 2010; S. Liu et al., 2011; C. Zhao et al., 2015) and biocompatibility (Y. Tu et al., 2013), presenting new opportunities for tissue engineering applications (S.H. Ku et al., 2013). GO nanomaterials can support the adhesion and proliferation of mammalian cells including human mesenchymal stem cells (hMSCs) (M. Kalbacova et al., 2010) human osteoblasts (Marie et al., 2012), fibroblasts (S.-R. Ryoo et al., 2010), and mammalian cells (O.N. Ruiz et al., 2011). The potential short-term and long-term toxicity of GO is a critical issue for their biomedical applications. However, GO did not show obvious toxicity at low concentrations (approx. 0-40 μg/ml) (Y. Chang et al., 2011). A low concentration GO film did not inhibit cell proliferation or differentiation in vitro, and enhanced biocompatibility and biodegradability. Consequently, GO is viewed as a prospective enhancing agent for augmenting PEO layers used in antibacterial and bone healing. Introducing GO into the calcium phosphate coating clearly impacts its biological characteristics (C. Santos et al., 2015; M. Li et al., 2014; Y.Y. Shi et al., 2016; Y. Zeng et al., 2016; Mao, Huanhuan et al., 2015).

Zhao (2016) et al. and Han (2017) et al. found that the corrosion resistance of the PEO coatings on AZ31 magnesium alloy was developed by introducing GO to the electrolyte during the PEO treatment. The incorporation of GO in the PEO coatings effectively decreased the number of micropores within the coatings (Figure 6). GO nanosheets can be seen in the pores, and the EIS result indicates that GO nanosheets have incorporated into the inner layer and the outer layer of the coating during PEO process. Other researchers have added graphene into PEO coating of Mg-Li (F. Chen et al., 2017) and Al (Q. Chen et al., 2017) alloy. The graphene-added PEO composite coating showed more uniform and compact with less structural defects compared with the PEO-based coating. Besides, the addition of graphene particles increased the PEO coating thickness and hardness. Yang (2016). et al. added GO in the PEO electrolyte for 6061 Al alloy. They found GO can improve the binding force, mechanical property and tribological behaviour.

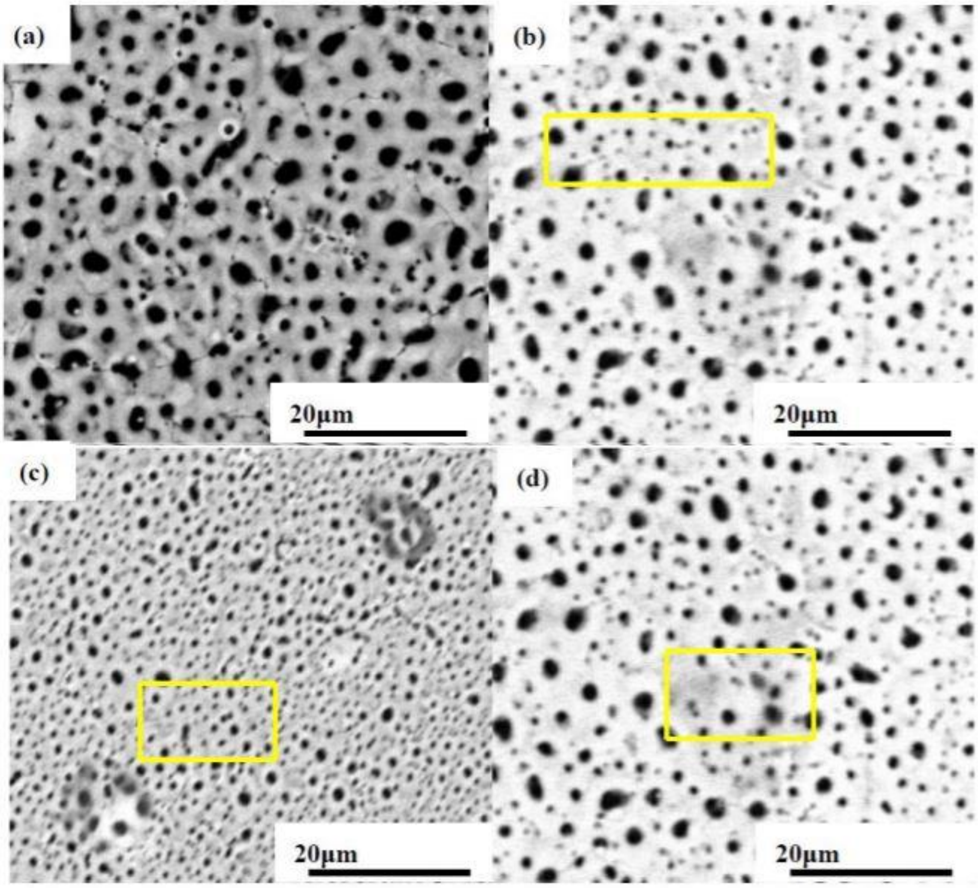

Figure 6. SEM surface morphology of the anodic oxidation coatings processed with a constant current density of 0.3 A cm^{-2} for 30 min in electrolytes containing 10 g/L of NaOH, 18 g/L of $Na_2SiO_3 \cdot 9H_2O$ with graphene additions of (a) 0, (b) 0.1 g/L, (c) 0.5 g/L and (d) 1.0 g/L (F. Chen et al., 2017)

Another advantage of GO is that its extraordinary surface has the largest adsorption capacity of chemical compounds including drugs, antibodies, proteins, and nucleic acids (such as aptamers) (N. Shadjou & M. Hasanzadeh, 2016; W. Chen et al., 2011). It means GO (or its reduction product) can easily compound with other nanoparticles like Ag (A. Janković et al., 2015; N. Kundu et al., 2017; S. Liu et al., 2017; S.B. Maddinedi et al., 2017; J. Zhao et al., 2014), Cu (W. Zhang et al., 2016), HA (C. Wen et al., 2017), $CaCO_3$ (S. Kim et al., 2011) or several different particles (Y. Zheng et al., 2017; J. Zhao et al., 2014). Compound particles may have multiple antibacterial functions, which express great potential for application. Wen (2017) et al. found that the suspended HA nanoparticles in the electrolyte could be successfully grafted on GO surface. The presence of HA/GO could seal the partial pores and decrease the diameter of some pores of the PEO coating (Figure 7). Thus, the corrosion resistance of the composite coating increases significantly.

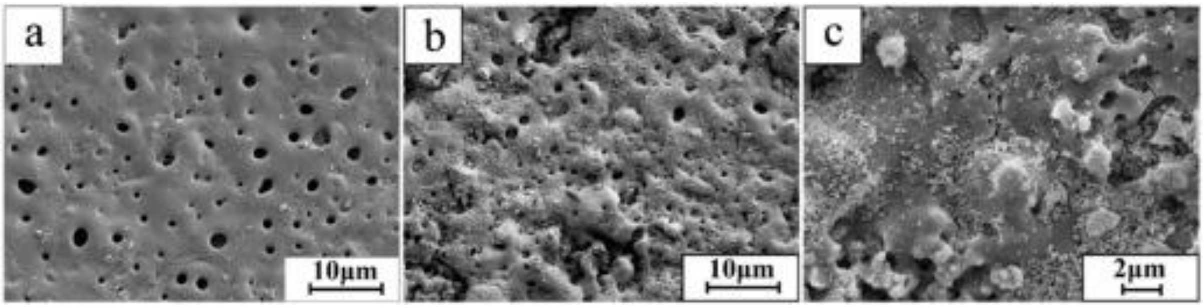

Figure 7. SEM morphologies of (a) PEO coating, (b) HA/GO coating, (c) high magnification image of HA/GO coating (C. Wen et al., 2017)

However, there is few report on the application of GO additive in the PEO electrolyte used for titanium alloy. Previous studies have focused on the effect of GO on the corrosion resistance of the PEO coating, but its influence on the biological properties has not been studied yet. Therefore, GO is a promising additive due to its ability to combine with other bioactive and antibacterial particles (HA, Ag, Cu, and Zn) and enhance multiple biological properties of the PEO coating. Graphene and its derivatives, like graphene oxide and reduced graphene oxide, are favored as additives in PEO composite coatings, favored for their durability in corrosive settings. Owing to their porous properties, graphene-family nanosheets can accumulate on PEO coatings, which significantly alter surface attributes (M. Pourshadloo et al., 2022). The team led by Yigit (O. Yigit et al., 2021) effectively developed nanoscale hydroxyapatite (nHA)-based coating fortified with graphene nanosheets (GNS) on Ti6Al4V alloys through the AC-PEO method. Findings indicate the feasibility of obtaining bioactive and hard layers via PEO in nHA/GNS solutions. As the weight percentage of GNS in the coating strata rose and the frequency of deposition elevated, the thickness and hardness of the coating also increased.

4. Temperature of Electrolyte

The research investigated the effect of electrolyte temperature changes on the formation of self-organized titanium oxide nanotube coating via anodic oxidation in titanium alloys. The study utilized electrolytic mixtures at varied temperatures, spanning from 5 to 70°C. The results showed that at a temperature of 25°C, significant outcomes were observed in the formation of TiO_2 nanotube arrays. These arrays had an average inner pore diameter of 125 nm, a length of 250 nm, a wall thickness of 30 nm, and an inter-tube space of 35 nm. The morphology of the nanotube arrays was smooth and circular, without any defects.

These findings suggest that controlling the temperature of the electrolyte is crucial for improving the quality of the film layer in plasma electrolytic oxidation. Higher temperatures enhance the dissolution energy, resulting in a thinner film layer and smaller resistance. The arcing voltage required also decreases with higher electrolyte's temperatures. Additionally, the conductivity of the electrolyte improves with temperature, leading to enhanced arc breakdown strength and increased pore diameter of the film layer.

Additionally, the film layer's roughness first rises before falling as the electrolyte temperature elevates. Under elevated temperatures, the quantity of holes on the specimen's surface rises, making the crossover between them increasingly noticeable. Consequently, this leads to a more level film layer and a reduction in crack count. In summary, the results underscore the significance of managing electrolyte temperature in plasma electrolytic oxidation to enhance the development of self-structured titanium oxide nanotube layers (L. Mohan et al., 2020).

5. Electrical Parameters

Factors like the power source, frequency, voltage, oxidation duration, and current density significantly affect the characteristics of PEO coatings. Given that these factors influence the microstructure, phase composition, and later the characteristics of PEO coatings, examining and refining these parameters is crucial. The intricate workings of the PEO process remain a mystery, yet the PEO coating deposition method is characterized as an electrochemical and electrothermal oxidation technique, influenced by micro discharges under optimal electrolytic circumstances (Y. Wang et al., 2015; X. Zhang et al., 2011; R.O. Hussein et al., 2010). Consequently, electrical factors like current/voltage features (including polarity, frequency, and duty cycle), as well as current density/voltage and oxidation time, have an indirect impact on phase development and are directly affected by the coating's density, growth speed, and efficiency (J. Ma et al., 2014; R.O. Hussein et al., 2012).

5.1 Power Source

It's been discovered that bipolar polarization enhances both the consistency and thickness of coatings (S.V. Gnedenkov et al., 2010). Large pores and imperfections arise from unipolar pulses, as gas becomes trapped within the coating, resulting in reduced resistance to corrosion (R.O. Hussein et al., 2012). The bipolar mechanism leads to briefer, more vigorous microdischarge occurrences, thereby producing coating with greater density and finer hardness, along with a reduced friction coefficient, in contrast to those formed using direct current (DC) mode (F. Jin et al., 2006; S. Wang et al., 2014). Yet, the coating applied in bipolar mode are 2.5 times denser, denser, and more consistent compared to those placed in unipolar mode. Consequently, it is broadly accepted that in the alternating current (AC) polarization mode, an anodic pulse propels oxidation reactions forward, and a cathodic pulse induces a sintering effect in the coating, leading to a denser surface and thus validating the process. Research (S. Xin et al., 2006) indicates that PEO coatings created with AC power generally surpass in quality, being harder and denser compared to those made under similar (anodic) DC conditions. Studies have also indicated that enhancing the quality of coatings occurs with the increase in cathodic voltage (Q. Li et al., 2014) or by boosting the cathodic to anodic current ratio (J.-H. Wang et al., 2014). However, the real processes during the cathodic half-cycle remain indistinct (S. Stojadinovic et al., 2015; A. Nominéet al., 2018; A.B. Rogov et al., 2017).

5.2 Frequency

Meanwhile, the effect of current and voltage frequency on coating morphology, chemical content, and phase composition was examined (A. Schwartz et al., 2022). Typically, plasma electrolytic oxidation (PEO) processing employs alternating current (AC) electricity at frequencies of 50 or 60 Hz. There is tremendous interest in changing this process in response to increased supply frequency. When a constant voltage is applied to the sample during PEO treatment, an increase in frequency has a significant impact on the localized current within it. Some experiments indicate a standard square wave voltage waveform for a single 50 Hz cycle (usually lasting 20 ms), with coating thicknesses of roughly 50 μm. Observations show that the anodic voltage exceeds 600 V, whereas the cathodic voltage is 125 V. When current profiles are investigated, both overall and for smaller area samples, it is discovered that, aside from brief early transient effects, the cumulative current is slightly greater than 2 A throughout both the anodic and cathodic half-cycles. As the supply frequency rises and the half-cycle period approaches the normal discharge lifespan, considerable variations in voltage and current patterns emerge. (As with the 50-Hz scenario, some cycles in the smaller sample show no discharges.) Notably, the cathodic voltage rises to over 250 V, a significant increase over the 125 V recorded at 50 Hz, while the anodic voltage stays around 600 V. The electrical profiles also demonstrate small alterations in the behavior of the cathodic phase, with discrete current pulses emerging alongside the continuous anodic discharges. Some of these pulses have larger current levels than anodic discharges, peaking at around 200 mA. Several investigations (W.-C. Gu, et al., 2007; H.-Y. Wang et al., 2013; B. Zou et al., 2015) have found that increasing the supply frequency (usually between 1.0 and 1.5 kHz) reduces coating growth rates, while reports on other effects differ (A. Yerokhin et al., 2016). It has also been observed that as the frequency increases, the microstructure of the coating becomes finer and more compact, which is typically considered favorable.

5.3 Voltage

Alicja (2019) et al. conducted a study on the PEO process using a $Ca(H_2PO_2)_2$ solution containing 150 g/dm^3 particles of hydroxyapatite. They found that favorable porous oxide layers were formed at 350 V and 450 V. By analyzing the samples with scanning electron microscopy (SEM), they observed that increasing the anodizing voltage resulted in a higher deposition rate and thickness of the oxide layer, as well as an increase in pore diameter (A. Kumar, 2022). It was further found that a maximum voltage of 315 V resulted in a more eco-friendly PEO method (L. Kostelac et al., 2022). Montazeri (2011) et al. studied an electrolyte solution contained 0.25 M CA and 0.025 M $NaH_2PO_4 \cdot 2H_2O$. When the treated time was fixed at 10 min, HA formation was only possible at the applied voltage of 500 V. At the voltage range of 350-450 V, porous layers containing titanium oxides which were mainly in the form of rutile and brookite, were produced (Figure 8).

In another study, the author investigated the influence of additive manufacturing (AM) on the wear resistance and morphology of PEO coatings on Ti-6Al-4V ELI alloy. Coatings were produced across three distinct voltage levels (200, 250, and 300 V). Investigations revealed that raising the voltage applied resulted in more roughness and larger pore spaces, alongside a reduction in the pore count of the coatings. Coatings produced at elevated voltages exhibited a markedly thicker thickness, ranging from 4.50 ± 0.33 to 23.83 ± 1.5 μm. Nonetheless, the coatings produced using lesser voltages featured slim, compact layers, leading to enhanced resistance to wear. The study concludes that the PEO process and voltage have a positive and promising impact on the properties of the coatings, making them suitable for applications in metallic implants (P.B. Santos et al., 2022).

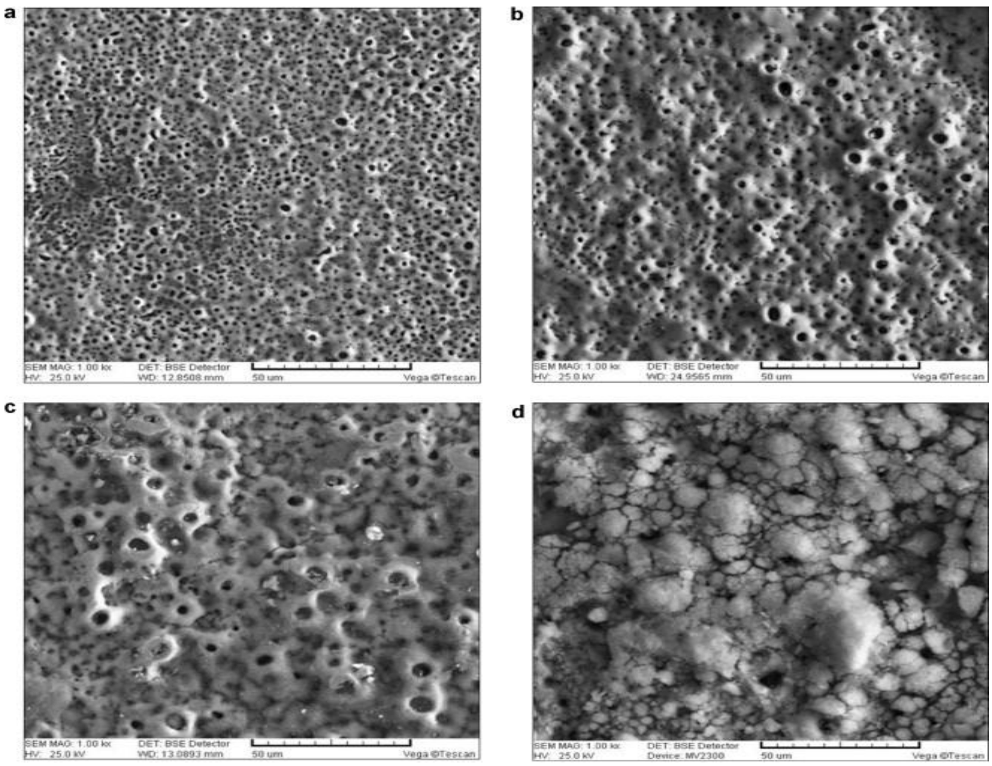

Figure 8. Surface SEM (1000×) of the coatings formed at different applied voltage (a) 350 V, (b) 400 V, (c) 450 V and (d) 500 V treated for 10 min (M. Montazeri et al., 2011)

5.4 Oxidation Time

The duration of treatment is equally crucial in shaping the depiction of PEO layers on Ti alloys. Cheng (2012) et al. discovered that micro-pore diameters expanded as the time for treatment rose from 1 minute to 30 minutes, in contrast to the count of these micro-pores on the coating's surface, which showed an inverse correlation with the duration of treatment. Fan (2012) and team synthesized the porous titanium layer using PEO on a low-voltage 90 V in H_2SO_4 electrolyte, applying the procedure for brief durations of 1, 2, and 3 minutes. Over time, the film's thickness escalates from 120 nm to 340 nm. In assessing apatite production in the SBF, it was determined that prolonged treatment correlates with apatite growth. Martínez Campos (2013) et al. conducted a comparative analysis between two electrolyte variants: A. 0.12 M CA and 0.01 M $(NaPO_3)_6$; B. 0.125 M CA and 0.025 M $NaH_2PO_4 \cdot 2H_2O$ electrolyte. The key distinction between type A and B coatings lies in the integration of Ca and P into the coatings. Extended exposure to electrolyte A for 600 seconds, with a coating layer 15 μm thick, leads to the creation of crystalline apatite, and the Ca/P ratio in this layer adheres to its stoichiometric composition (1.5-1.7). In contrast, electrolyte B results in layers with an excessively high Ca/P ratio, escalating over time from 2.0 to 4.0 in the case of coatings 5 μm and 15 μm in thickness, respectively. Additionally, both Ca and P are evenly dispersed over the A-type coatings and primarily situated in the exterior segment (around the top ~3 μm) of the B coatings. There was a reduction in the number of pores, whereas the dimensions of the cracks, pores, and the surface texture escalated as PEO time extended (S. Durdu et al., 2013). Prolonged exposure may result in fractures caused by thermal pressures in Photothermal Energy Transfer. As the treatment time increased, the porosity of films reduced and the thickness increased; meanwhile the relative contents of Ca and P unchanged but the hydroxyapatite became a predominant component when the treatment time was 30 or 40 min (V. K et al., 2013). And in the meanwhile, the adhesion strengths of the PEO coatings are enhanced with the increasing voltage and time (P. Behzad et al., 2022).

5.5 Current Density

Literature analysis reveals that a consistent current density approach is commonly employed to enhance the regulation of oxidation processes. The microstructure and characteristics of the coated material are significantly affected by the density of the current. For instance, different current densities were administered to unadulterated titanium to study the workings of PEO. In the PEO phases, the study of the growth dynamics and oxide traits involved examining the effects of ionic and electronic currents. Observations indicated that with reduced current density levels (30 and 40 mA/cm^2), electronic currents prevailed, leading to greater porosity and roughness on the coating. With the rise in current density, the inclusion of ionic current escalated, resulting in the creation of thick anatomical layers. Achieving peak growth rates was possible in the equilibrium of ionic and electronic charges. Furthermore, maintaining a steady current density resulted in a rise in spark discharge intensity and a reduction in spark discharge numbers over extended process durations (G. Mortazavi et al., 2019).

As reported by Srinivasan (2013) et al. and Wolke (2003) et al. the thickness of the coating grows almost directly in correlation with the growing current density. Consequently, as the current density rises for the treatment period, the coatings' roughness and porosity/defect rates expand, mainly due to the enlarged scale of the discharge event (G.-l. Yang et al., 2009). The amount of phase content varies alongside the density of the current. Yang (2012) et al. developed a PEO layer, consisting of both anatase and rutile phases. A rise in current density resulted in a higher concentration of rutile. The outcome aligns with the research conducted by Dong Hyuk Shin (K.R. Shin et al., 2014). The research indicated an increase in pore sizes correlating with higher current density, alongside a reduction in both roughness and anatase levels. The vitro tests showed that the coating prepared at the lower current density has an advantage in inducing biomimetic apatite formation and cell proliferation. Anatase is known to be more suitable for apatite formation than rutile (Masaki et al., 2003; S. Aliasghari et al., 2014).

Lederer (2021) et al. discovered that wear-resistant coatings are also influenced by current density. The study showed that elevating current density and frequency caused the creation of coatings that are both mechanically firm and sticky, inclusive of corundum and zirconia, enhancing their tribological characteristics. Therefore, the primary factors responsible for generating wear-resistant coatings are current density and repetition rate. Anodic current density can be increased by raising the applied voltage and the temperature of the electrolyte (A. Kumar, 2022). To achieve better results in the PEO process, permitting free decay of current density in its latter phase is advantageous. This method lessens the force of spark discharges and fosters the creation of tiny sparks that are evenly spread over the oxide layer's entire surface. Under these conditions, coatings demonstrate enhanced stability, comparative ease, and a uniform microstructure characterized by decreased porosity (C. Schouten et al., 2010; J. Liang et al., 2007). Furthermore, increasing the cathode current density has been found to enhance coating compactness and improve corrosion resistance (Y. Wang et al., 2004; X. Sun et al., 2005).

A concise summary of electrical parameters reveals a clear advantage of AC power for the PEO process, particularly with an increased cathodic to anodic current ratio. Higher current density leads to larger pore size and higher rutile content, which are less effective in inducing biomimetic apatite formation and cell proliferation compared to the anatase phase. The porosity, crack size, pore size, and surface roughness change over oxidation time, while crystallinity increases with time. The effect of frequency on PEO coating remains contradictory. It should also be noted that the electrical parameters of the PEO process are partly dependent on the applied electrolyte.

6. Conclusion

In conclusion, our findings indicate that PEO is often used in crafting Ca-P coatings on Ti-based biomaterials, due to its superior efficiency and cost-effectiveness, unlike other synthesis methods. Meanwhile, a number of variables that directly affect the tangible and chemical characteristics of Ca-P coatings produced with PEO, including electrolyte composition, additives, and the used electrical parameters. Additionally, by adjusting the Ca/P ratio in the electrolyte, efficient generation of bioactive hydroxyapatite coatings becomes achievable. Moreover, given that calcium acetate can support arc discharge at reduced current densities, it is often employed as the calcium component in electrolytes. Besides, there will be more calcium in the uniform porous covering. Furthermore, owing to its antibacterial properties and its ability to synergize with other bioactive and antibacterial agents such as HA, Ag, Cu, and Zn, adding GO is beneficial. Consequently, the PEO process and the coating's biocompatibility can both be enhanced by the addition of other elements, such as Si, to the electrolyte. A superior performance of oxide coatings can be prepared by selecting the right electrolyte temperature. It is advantageous to produce coatings with fewer pores, no cracks, and smooth surface morphology when the electrolyte temperature is low. Furthermore, AC power is advantageous in the process of fabricating PEO coatings, particularly when the cathodic current is raised. Greater surface roughness and greater fracture and pore diameters are caused by longer oxidation times. Additionally, the coating's microstructure gets denser and finer as the power output frequency rises. Simultaneously, when current density increases, the content of anatase declines, as it is less effective in triggering biomimetic apatite synthesis and cell growth. PEO, in conclusion, improves coating thickness and wear resistance, positioning it as an effective method for producing Ca-P coatings on Ti-based implants. Altering the thickness and shape of PEO layers using calcium phosphate enhances both the biocompatibility and bone integration of metal biomaterials.

References

A. Fattah-alhosseini, M. Molaei, K. Babaei, (2020). The effects of nano- and micro-particles on properties of plasma electrolytic oxidation (PEO) coatings applied on titanium substrates: A review. *Surfaces and*

Interfaces, *21*, 100659.

A. Janković, S. Eraković, M. Vukašinović-Sekulić, V. Mišković-Stanković, S.J. Park, K.Y. Rhee, (2015). Graphene-based antibacterial composite coatings electrodeposited on titanium for biomedical applications. *Progress in Organic Coatings*, *83*, 1-10.

A. Kazek-Kęsik, M. Krok-Borkowicz, E. Pamuła, W. Simka, (2014). Electrochemical and biological characterization of coatings formed on Ti–15Mo alloy by plasma electrolytic oxidation. *Materials Science and Engineering: C*, *43*, 172-181.

A. Kossenko, S. Lugovskoy, N. Astashina, A. Lugovskoy, M. Zinigrad, (2013). Effect of time on the formation of hydroxyapatite in PEO process with hydrothermal treatment of the Ti-6Al-4V alloy. *Glass Physics & Chemistry*.

A. Kumar, (2022). Anodization of Titanium Alloy (Grade 5) to Obtain Nanoporous Surface Using Sulfuric Acid Electrolyte. *IETE Journal of Research*, *68*(5), 3855-3861.

A. Lugovskoy, S. Lugovskoy, (2014). Production of hydroxyapatite layers on the plasma electrolytically oxidized surface of titanium alloys. *Materials Science & Engineering. C*, *43*, 527-532.

A. Nominé, A.V. Nominé, N.S. Braithwaite, T. Belmonte, G. Henrion, (2018). High-frequency induced cathodic breakdown during plasma electrolytic oxidation. *Phys. Rev. Applied*.

A. Schwartz, A. Kossenko, M. Zinigrad, Y. Gofer, K. Borodianskiy, A. Sobolev, (2022). Hydroxyapatite Coating on Ti-6Al-7Nb Alloy by Plasma Electrolytic Oxidation in Salt-Based Electrolyte. *Materials*.

A. Sobolev, A. Valkov, A. Kossenko, I. Wolicki, K. Borodianskiy, (2019). Bioactive Coating on Ti Alloy with High Osseointegration and Antibacterial Ag Nanoparticles. *ACS Applied Materials & Interfaces*, *2019*(XXXX).

A. Yerokhin, E.V. Parfenov, A. Matthews, (2016). In situ impedance spectroscopy of the plasma electrolytic oxidation process for deposition of Ca- and P-containing coatings on Ti. *Surface and Coatings Technology*, *301*, 54-62.

A.B. Rogov, A. Yerokhin, A. Matthews, (2017). The Role of Cathodic Current in Plasma Electrolytic Oxidation of Aluminum: Phenomenological Concepts of the “Soft Sparking” Mode. *Langmuir*, *33*(41), 11059-11069.

A.R. Rafieerad, M.R. Ashra, R. Mahmoodian, A.R. Bushroa, (2015). Surface characterization and corrosion behavior of calcium phosphate-base composite layer on titanium and its alloys via plasma electrolytic oxidation: A review paper. *Materials Science & Engineering. C*, *57*, 397-413.

B. Han, Y. Yang, Z. Huang, L. You, H. Huang, K. Wang, (2017). A Composite Anodic Coating Containing Graphene on AZ31 Magnesium Alloy. *International Journal of Electrochemical Science*, *12*(10), 9829-9843.

B. He, C. Xin, Y. Chen, Y. Xu, Q. Zhao, Z. Hou, Y. Tang, H. Liu, X. Su, Y. Zhao, (2022). Biological performance and tribocorrosion behavior of in-situ synthesized CuxO/TiO2 coatings. *Applied Surface Science*, *600*, 154096.

B. Zou, G.-h. LÜ, G.-l. Zhang, Y.-y. Tian, (2015). Effect of current frequency on properties of coating formed by microarc oxidation on AZ91D magnesium alloy. *Transactions of Nonferrous Metals Society of China*, *25*(5), 1500-1505.

B.S. Necula, I. Apachitei, F.D. Tichelaar, L.E. Fratila-Apachitei, J. Duszczyk, (2011). An electron microscopical study on the growth of TiO2–Ag antibacterial coatings on Ti6Al7Nb biomedical alloy. *Acta Biomaterialia*, *7*(6), 2751-2757.

B.S. Necula, J.P.T.M. van Leeuwen, L.E. Fratila-Apachitei, S.A.J. Zaat, I. Apachitei, J. Duszczyk, (2012). In vitro cytotoxicity evaluation of porous TiO2–Ag antibacterial coatings for human fetal osteoblasts. *Acta Biomaterialia*, *8*(11), 4191-4197.

B.S. Necula, L.E. Fratila-Apachitei, S.A.J. Zaat, I. Apachitei, J. Duszczyk, (2009). In vitro antibacterial activity of porous TiO2–Ag composite layers against methicillin-resistant Staphylococcus aureus. *Acta Biomaterialia*, *5*(9), 3573-3580.

C. Santos, C. Piedade, P.J. Uggowitzer, M.F. Montemor, M.J. Carmezim, (2015). Parallel nano-assembling of a multifunctional GO/HapNP coating on ultrahigh-purity magnesium for biodegradable implants. *Applied Surface Science*, *345*, 387-393.

C. Schouten, G.J. Meijer, J.J.J.P. van den Beucken, S.C.G. Leeuwenburgh, L.T. de Jonge, J.G.C. Wolke, P.H.M. Spauwen, J.A. Jansen, (2010). In vivo bone response and mechanical evaluation of electrosprayed CaP nanoparticle coatings using the iliac crest of goats as an implantation model. *Acta Biomaterialia*, *6*(6), 2227-2236.

C. Wen, X. Zhan, X. Huang, F. Xu, L. Luo, C. Xia, (2017). Characterization and corrosion properties of hydroxyapatite/graphene oxide bio-composite coating on magnesium alloy by one-step micro-arc oxidation method. *Surface and Coatings Technology*, *317*, 125-133.

C. Zhao, X. Lu, C. Zanden, J. Liu, (2015). The promising application of graphene oxide as coating materials in orthopedic implants: preparation, characterization and cell behavior. *Biomedical Materials*, *10*(1), 015019.

C.A. Antônio, E.C. Rangel, S.F. Durrant, A.D.O. Delgado-Silva, M.H. Tabacniks, N.C.D. Cruz, (2017). Mg-Containing Hydroxyapatite Coatings Produced by Plasma Electrolytic Oxidation of Titanium. *Materials Research*, *20*(4), 891-898.

C.J. Chung, R.T. Su, H.J. Chu, H.T. Chen, H.K. Tsou, J.L. He, (2013). Plasma electrolytic oxidation of titanium and improvement in osseointegration. *Journal of Biomedical Materials Research Part B Applied Biomaterials*, *101B*(6), 1023-1030.

D. Krupa, J. Baszkiewicz, J. Zdunek, J.W. Sobczak, Z. Somka, (2012). Effect of plasma electrolytic oxidation in the solutions containing Ca, P, Si, Na on the properties of titanium. *Journal of Biomedical Materials Research Part B Applied Biomaterials*, *100*(8), 2156-2166.

D. Quintero, O. Galvis, J.A. Calderón, M.A. Gómez, J.G. Castaño, F. Echeverría, H. Habazaki, (2015). Control of the physical properties of anodic coatings obtained by plasma electrolytic oxidation on Ti6Al4V alloy. *Surface and Coatings Technology*, *283*, 210-222.

D.-Y. Kim, M. Kim, H.-E. Kim, Y.-H. Koh, H.-W. Kim, J.-H. Jang, (2009). Formation of hydroxyapatite within porous TiO2 layer by micro-arc oxidation coupled with electrophoretic deposition. *Acta Biomaterialia*, *5*(6), 2196-2205.

F. Chen, Y. Zhang, Y. Zhang, (2017). Effect of Graphene on Micro-Structure and Properties of MAO Coating Prepared on Mg-Li Alloy. *International Journal of Electrochemical Science*, *12*(7), 6081-6091.

F. Jin, P.K. Chu, G. Xu, J. Zhao, D. Tang, H. Tong, (2006). Structure and mechanical properties of magnesium alloy treated by micro-arc discharge oxidation using direct current and high-frequency bipolar pulsing modes. *Materials Science and Engineering: A*, *435-436*, 123-126.

F. Liu, F. Wang, T. Shimizu, K. Igarashi, L. Zhao, (2005). Formation of hydroxyapatite on Ti–6Al–4V alloy by microarc oxidation and hydrothermal treatment. *Surface and Coatings Technology*, *199*(2), 220-224.

F. Simchen, M. Sieber, A. Kopp, T. Lampke, (2020). Introduction to Plasma Electrolytic Oxidation — An Overview of the Process and Applications. *Coatings*.

G. Mortazavi, J. Jiang, E.I. Meletis, (2019). Investigation of the plasma electrolytic oxidation mechanism of titanium. *Applied Surface Science*, *488*, 370-382.

G.-l. Yang, F.-m. He, J.-a. Hu, X.-x. Wang, S.-f. Zhao, (2009). Effects of biomimetically and electrochemically deposited nano-hydroxyapatite coatings on osseointegration of porous titanium implants. *Oral Surgery, Oral Medicine, Oral Pathology, Oral Radiology, and Endodontology*, *107*(6), 782-789.

H. Hu, W. Zhang, Y. Qiao, X. Jiang, X. Liu, C. Ding, (2012). Antibacterial activity and increased bone marrow stem cell functions of Zn-incorporated TiO2 coatings on titanium. *Acta Biomaterialia*, *8*(2) 904-915.

H. Sharifi, M. Aliofkhazraei, G.B. Darband, A.S. Rouhaghdam, (2016). Characterization of PEO nanocomposite coatings on titanium formed in electrolyte containing atenolol. *Surface and Coatings Technology*, *304*, 438-449.

H. Shi, D. Liu, X. Zhang, W. Zhao, Z. Liu, M. Li, Y.J.M. He, (2021). Corrosion, Effect of plasma electrolytic oxidation on the hot salt corrosion fatigue behavior of the TC17 titanium alloy. *Materials and Corrosion*.

H.-T. Chen, C.-J. Chung, T.-C. Yang, I.P. Chiang, C.-H. Tang, K.-C. Chen, J.-L. He, (2010). Osteoblast growth behavior on micro-arc oxidized β-titanium alloy. *Surface and Coatings Technology*, *205*(5), 1624-1629.

H.-Y. Wang, R.-F. Zhu, Y.-P. Lu, G.-Y. Xiao, J.I.E. Ma, Y.F. Yuan, (2013). PREPARATION AND MECHANISM OF CONTROLLABLE MICROPORES ON BIOCERAMIC TiO2 COATINGS BY PLASMA ELECTROLYTIC OXIDATION. *Surface Review and Letters*, *20*(05), 1350051.

H.-Y. Wang, R.-F. Zhu, Y.-P. Lu, G.-Y. Xiao, X.-C. Zhao, K. He, Y.F. Yuan, Y. Li, X.-N. Ma, (2014). Preparation and properties of plasma electrolytic oxidation coating on sandblasted pure titanium by a combination treatment. *Materials Science and Engineering: C*, *42*, 657-664.

Hongshan San, Jin Hu, Yufen Zhang, Jiaping Han and Shawei Tang, (2017). Corrosion Behavior of Cathodic Electrodeposition Coatings on Micro-Arc Oxidized Titanium Alloy in Simulated Body Fluid. *Journal of*

The Electrochemical Society.

I.A.J. van Hengel, M. Riool, L.E. Fratila-Apachitei, J. Witte-Bouma, E. Farrell, A.A. Zadpoor, S.A.J. Zaat, I. Apachitei, (2017). Selective laser melting porous metallic implants with immobilized silver nanoparticles kill and prevent biofilm formation by methicillin-resistant Staphylococcus aureus. *Biomaterials*, *140*, 1-15.

I.A.J. Van Hengel, M.W.A.M. Tierolf, L.E. Fratilaapachitei, I. Apachitei, A.A. Zadpoor, (2021). Antibacterial Titanium Implants Biofunctionalized by Plasma Electrolytic Oxidation with Silver, Zinc, and Copper: A Systematic Review. *International journal of molecular sciences*, *22*(7), 3800.

J. Chen, Q. Guo, W.X. Yang, Dapeng, (2024). Effects of Micro-arc Oxidation/Multi-arc Ion Plating Composite Treatment on Microstructure and Properties of TC4 Titanium Alloy. *Journal of Materials Engineering and Performance*, *33*(3), 1391-1400.

J. Hadzik, K. Jurczyszyn, T. Gębarowski, A. Trytek, T. Gedrange, M. Kozakiewicz, M. Dominiak, P. Kubasiewicz-Ross, A. Trzcionka-Szajna, E. Szajna, W. Simka, (2023). An Experimental Anodized and Low-Pressure Oxygen Plasma-Treated Titanium Dental Implant Surface — Preliminary Report. *International Journal of Molecular Sciences*.

J. Liang, B. Guo, J. Tian, H. Liu, J. Zhou, T. Xu, (2005). Effect of potassium fluoride in electrolytic solution on the structure and properties of microarc oxidation coatings on magnesium alloy. *Applied Surface Science*, *252*(2), 345-351.

J. Liang, L. Hu, J. Hao, (2007). Improvement of corrosion properties of microarc oxidation coating on magnesium alloy by optimizing current density parameters. *Applied Surface Science*, *253*(16), 6939-6945.

J. Ma, Y.S. Yang, X.C. Wang, J. Zhang, S. Liu, X.B. Yi, (2014). Effect of Impulse Voltage on Microstructure and Corrosion Resistance of Microarc Oxidation Coatings on AZ80 Magnesium Alloy. *Key Engineering Materials*, *575-576*, 418-422.

J. Michalska, M. Sowa, M. Piotrowska, M. Widziołek, G. Tylko, G. Dercz, R.P. Socha, A.M. Osyczka, W. Simka, (2019). Incorporation of Ca ions into anodic oxide coatings on the Ti-13Nb-13Zr alloy by plasma electrolytic oxidation. *Materials Science & Engineering. C*, *104*, 109957.

J. Sun, Y. Han, X. Huang, (2007). Hydroxyapatite coatings prepared by micro-arc oxidation in Ca- and P-containing electrolyte. *Surface and Coatings Technology*, *201*(9), 5655-5658.

J. Zhao, X. Xie, C. Zhang, (2016). Effect of the Graphene Oxide Additive on the Corrosion Resistance of the Plasma Electrolytic Oxidation Coating of the AZ31 Magnesium Alloy. *Corrosion science*, *114*(JAN.) 146-155.

J. Zhao, Z. Zhang, Z. Yu, S. Yang, H. Jiang, (2014). Synthesis of hydroxyapatite on thioglycolic acid-capped reduced graphene oxide/silver nanoparticles: Effect of reaction condition in normal or pathological simulated body fluid. *Materials Letters*, *116*, 359-362.

J. Zhao, Z. Zhang, Z. Yu, Z. He, S. Yang, H. Jiang, (2014). Nucleation and characterization of hydroxyapatite on thioglycolic acid-capped reduced graphene oxide/silver nanoparticles in simplified simulated body fluid. *Applied Surface Science*, *289*, 89-96.

J.G.C. Wolke, J.P.C.M. van der Waerden, H.G. Schaeken, J.A. Jansen, (2003). In vivo dissolution behavior of various RF magnetron-sputtered Ca-P coatings on roughened titanium implants. *Biomaterials*, *24*(15), 2623-2629.

J.-H. Ni, Y.-L. Shi, F.-Y. Yan, J.-Z. Chen, L. Wang, (2008). Preparation of hydroxyapatite-containing titania coating on titanium substrate by micro-arc oxidation. *Materials Research Bulletin*, *43*(1), 45-53.

J.-H. Wang, M.-H. Du, F.-Z. Han, J. Yang, (2014). Effects of the ratio of anodic and cathodic currents on the characteristics of micro-arc oxidation ceramic coatings on Al alloys. *Applied Surface Science*, *292*, 658-664.

J.R. Henstock, L.T. Canham, S.I. Anderson, (2015). Silicon: The evolution of its use in biomaterials. *Acta Biomaterialia*, *11*, 17-26.

J.-z. Chen, Y.-l. Shi, L. Wang, F.-y. Yan, F.-q. Zhang, (2006). Preparation and properties of hydroxyapatite-containing titania coating by micro-arc oxidation. *Materials Letters*, *60*(20), 2538-2543.

K. Rokosz, T. Hryniewicz, K. Pietrzak, P. Sadlak, J. Valíek, (2017). Fabrication and characterisation of porous, calcium enriched coatings on titanium after plasma electrolytic oxidation under DC regime. *Advances in Materials Science*, *17*(4).

K. Venkateswarlu, N. Rameshbabu, D. Sreekanth, A.C. Bose, V. Muthupandi, S. Subramanian, (2013). Fabrication and characterization of micro-arc oxidized fluoride containing titania films on Cp Ti. *Ceramics*

International, *39*(1), 801-812.

K.R. Shin, Y.G. Ko, D.H. Shin, (2011). Effect of electrolyte on surface properties of pure titanium coated by plasma electrolytic oxidation. *Journal of Alloys and Compounds*, *509*, S478-S481.

K.R. Shin, Y.S. Kim, H.W. Yang, Y.G. Ko, D.H. Shin, (2014). In vitro biological response to the oxide layer in pure titanium formed at different current densities by plasma electrolytic oxidation. *Applied Surface Science*, *314*, 221-227.

L. Kostelac, L. Pezzato, A.G. Settimi, M. Franceschi, C. Gennari, K. Brunelli, C. Rampazzo, M. Dabalà, (2022). Investigation of hydroxyapatite (HAP) containing coating on grade 2 titanium alloy prepared by plasma electrolytic oxidation (PEO) at low voltage. *Surfaces and Interfaces*, *30*, 101888.

L. Mohan, C. Dennis, N. Padmapriya, C. Anandan, N. Rajendran, (2020). Effect of Electrolyte Temperature and Anodization Time on Formation of TiO2 Nanotubes for Biomedical Applications. *Materials Today Communications*, *23*, 101103.

L. Wang, L. Shi, J. Chen, Z. Shi, L. Ren, Y. Wang, (2014). Biocompatibility of Si-incorporated TiO2 film prepared by micro-arc oxidation. *Materials Letters*, *116*, 35-38.

M. Aliofkhazraei, R.S. Gharabagh, M. Teimouri, M. Ahmadzadeh, G.B. Darband, H. Hasannejad, (2016). Ceria embedded nanocomposite coating fabricated by plasma electrolytic oxidation on titanium. *Journal of Alloys and Compounds*, *685*, 376-383.

M. Kalbacova, A. Broz, J. Kong, M. Kalbac, (2010). Graphene substrates promote adherence of human osteoblasts and mesenchymal stromal cells. *Carbon*, *48*(15), 4323-4329.

M. Kaseem, H.-C. Choe, (2021). Acceleration of Bone Formation and Adhesion Ability on Dental Implant Surface via Plasma Electrolytic Oxidation in a Solution Containing Bone Ions. *Metals*.

M. Kaseem, H.-C. Choe, (2021). Simultaneous improvement of corrosion resistance and bioactivity of a titanium alloy via wet and dry plasma treatments. *Journal of Alloys and Compounds*, *851*, 156840.

M. Li, Q. Liu, Z. Jia, X. Xu, Y. Cheng, Y. Zheng, T. Xi, S. Wei, (2014). Graphene oxide/hydroxyapatite composite coatings fabricated by electrophoretic nanotechnology for biological applications. *Carbon*, *67*, 185-197.

M. Montazeri, C. Dehghanian, M. Shokouhfar, A. Baradaran, (2011). Investigation of the voltage and time effects on the formation of hydroxyapatite-containing titania prepared by plasma electrolytic oxidation on Ti–6Al–4V alloy and its corrosion behavior. *Applied Surface Science*, *257*(16), 7268-7275.

M. Pourshadloo, H.A. Rezaei, M. Saeidnia, H. Alkokab, M.S. Bathaei, (2022). Effect of g-family incorporation on corrosion behavior of PEO-treated titanium alloys: a review. *Surface Innovations*, *11*(1-3), 5-14.

M. Qadir, Y. Li, K. Munir, C. Wen, (2017). Calcium Phosphate-Based Composite Coating by Micro-Arc Oxidation (MAO) for Biomedical Application: A Review. *Critical Reviews in Solid State & Material Sciences*, 1-25.

M. Sowa, A. Kazek-Kęsik, R.P. Socha, G. Dercz, J. Michalska, W. Simka, (2013). Modification of tantalum surface via plasma electrolytic oxidation in silicate solutions. *Electrochimica Acta*, *114*, 627-636.

M.-A. Faghihi-Sani, A. Arbabi, A. Mehdinezhad-Roshan, (2013). Crystallization of hydroxyapatite during hydrothermal treatment on amorphous calcium phosphate layer coated by PEO technique. *Ceramics International*, *39*(2), 1793-1798.

M.-S. Kim, J.-J. Ryu, Y.-M. Sung, (2007). One-step approach for nano-crystalline hydroxyapatite coating on titanium via micro-arc oxidation. *Electrochemistry Communications*, *9*(8), 1886-1891.

Mao, Huanhuan, Yan, Yajing, Ding, Qiongqiong, Huang, Yong, Zhang, Xuejiao, (2015). Hydroxyapatite/gelatin functionalized graphene oxide composite coatings deposited on TiO2 nanotube by electrochemical deposition for biomedical applications. *Applied Surface Science*.

Marie, Kalbacova, Antonin, Broz, Martin, Kalbac, (2012). Influence of the fetal bovine serum proteins on the growth of human osteoblast cells on graphene. *Journal of Biomedical Materials Research Part A*, *100A*(11), 3001-3007.

Masaki, Uchida, Hyun-Min, Kim, Tadashi, Kokubo, Shunsuke, Fujibayashi, Takashi, Nakamura, (2003). Structural dependence of apatite formation on titania gels in a simulated body fluid. *Journal of Biomedical Materials Research Part A*.

N. Iqbal, M.R.A. Kadir, N.H. Mahmood, N. Salim, G.R.A. Froemming, H.R. Balaji, T. Kamarul, (2014). Characterization, antibacterial and in vitro compatibility of zinc–silver doped hydroxyapatite nanoparticles prepared through microwave synthesis. *Ceramics International*, *40*(3), 4507-4513.

N. Kundu, D. Mukherjee, T.K. Maiti, N. Sarkar, (2017). Protein-Guided Formation of Silver Nanoclusters and Their Assembly with Graphene Oxide as an Improved Bioimaging Agent with Reduced Toxicity. *The Journal of Physical Chemistry Letters*, *8*(10), 2291-2297.

N. Shadjou, M. Hasanzadeh, (2016). Graphene and its nanostructure derivatives for use in bone tissue engineering: Recent advances. *Journal of Biomedical Materials Research Part A*, *104*(5), 1250-1275.

N.A. Sukrey, M. Rizwan, A.R. Bushroa, S.Z. Salleh, W.J. Basirun, (2021). Development and characterization of bioglass incorporated plasma electrolytic oxidation layer on titanium substrate for biomedical application. *REVIEWS ON ADVANCED MATERIALS SCIENCE*, *60*(1), 678-690.

O. Oleshko, I. Liubchak, Y. Husak, V. Korniienko, A. Yusupova, T. Oleshko, R. Banasiuk, M. Szkodo, I. Matros-Taranets, A. Kazek-Kęsik, W. Simka, M. Pogorielov, (2020). In Vitro Biological Characterization of Silver-Doped Anodic Oxide Coating on Titanium. *Materials*.

O. Yigit, B. Dikici, N. Ozdemir, E. Arslan, (2021). Plasma electrolytic oxidation of Ti-6Al-4V alloys in nHA/GNS containing electrolytes for biomedical applications: The combined effect of the deposition frequency and GNS weight percentage. *Surface and Coatings Technology*, *415*, 127139.

O.N. Ruiz, K.A.S. Fernando, B. Wang, N.A. Brown, P.G. Luo, N.D. McNamara, M. Vangsness, Y.-P. Sun, C.E. Bunker, (2011). Graphene Oxide: A Nonspecific Enhancer of Cellular Growth. *ACS Nano*, *5*(10), 8100-8107.

P. Behzad, A. Vahid, B. Omid, K.R. Banafsheh, (2022). Thermomechanical and Plasma Electrolytic Oxidation Processes Evaluation for a Beta Ti-Nb-Zr-Ta Alloy. *Journal of Materials Engineering and Performance*.

P.B. Santos, E.K. Baldin, D.A. Krieger, V.V. de Castro, C. Aguzzoli, J.C. Fonseca, M. Rodrigues, M.A. Lopes, C.D.F. Malfatti, (2021). Wear performance and osteogenic differentiation behavior of plasma electrolytic oxidation coatings on Ti-6Al-4V alloys: Potential application for bone tissue repairs. *Surface and Coatings Technology*, *417*, 127179.

P.B. Santos, V.V. de Castro, E.K. Baldin, C. Aguzzoli, G.A. Longhitano, A.L. Jardini, É.S. Lopes, A.M. de Andrade, C. de Fraga Malfatti, (2022). Wear Resistance of Plasma Electrolytic Oxidation Coatings on Ti-6Al-4V Eli Alloy Processed by Additive Manufacturing. *Metals*.

P.N. Belkin, S.A. Kusmanov, A.V. Zhirov, V.S. Belkin, V.I. Parfenyuk, (2016). Anode Plasma Electrolytic Saturation of Titanium Alloys with Nitrogen and Oxygen. *Journal of Materials Science & Technology*, *32*(10), 1027-1032.

Q. Chen, Z. Jiang, S. Tang, W. Dong, Q. Tong, W. Li, (2017). Influence of graphene particles on the micro-arc oxidation behaviors of 6063 aluminum alloy and the coating properties. *Applied Surface Science*, *423*, 939-950.

Q. Li, J. Liang, B. Liu, Z. Peng, Q. Wang, (2014). Effects of cathodic voltages on structure and wear resistance of plasma electrolytic oxidation coatings formed on aluminium alloy. *Applied Surface Science*, *297*, 176-181.

R. Luo, Z. Liu, F. Yan, Y. Kong, Y. Zhang, (2013). The biocompatibility of hydroxyapatite film deposition on micro-arc oxidation Ti6Al4V alloy. *Applied Surface Science*, *266*, 57-61.

R. Zhou, D. Wei, H. Ke, J. Cao, B. Li, S. Cheng, W. Feng, Y. Wang, D. Jia, Y. Zhou, (2015a). H2Ti5O11 center dot H2O nanorod arrays formed on a Ti surface via a hybrid technique of microarc oxidation and chemical treatment. *CrystEngComm*, *17*(13).

R. Zhou, D. Wei, H. Yang, S. Cheng, W. Feng, B. Li, Y. Wang, D. Jia, Y. Zhou, (2014e). Osseointegration of bioactive microarc oxidized amorphous phase/TiO2 nanocrystals composited coatings on titanium after implantation into rabbit tibia. *Journal of Materials Science: Materials in Medicine*, *25*(5), 1307-1318.

R. Zhou, D. Wei, H. Yang, W. Feng, S. Cheng, B. Li, Y. Wang, D. Jia, Y. Zhou, (2014c). MC3T3-E1 cell response of amorphous phase/TiO2 nanocrystal composite coating prepared by microarc oxidation on titanium. *Materials Science and Engineering: C*, *39*, 186-195.

R. Zhou, D. Wei, J. Cao, W. Feng, S. Cheng, Q. Du, B. Li, Y. Wang, D. Jia, Y. Zhou, (2015b). The effect of NaOH concentration on the steam-hydrothermally treated bioactive microarc oxidation coatings containing Ca, P, Si and Na on pure Ti surface. *Materials Science and Engineering: C*, *49*, 669-680.

R. Zhou, D. Wei, S. Cheng, B. Li, Y. Wang, D. Jia, Y. Zhou, H. Guo, (2014a). The structure and in vitro apatite formation ability of porous titanium covered bioactive microarc oxidized TiO2-based coatings containing Si, Na and Ca. *Ceramics International*, *40*(1, Part A), 501-509.

R. Zhou, D. Wei, S. Cheng, W. Feng, Q. Du, H. Yang, B. Li, Y. Wang, D. Jia, Y. Zhou, (2014d). Structure, MC3T3-E1 Cell Response, and Osseointegration of Macroporous Titanium Implants Covered by a Bioactive Microarc Oxidation Coating with Microporous Structure. *ACS Applied Materials & Interfaces*, *6*(7), 4797-4811.

R. Zhou, D. Wei, W. Feng, S. Cheng, H. Yang, B. Li, Y. Wang, D. Jia, Y. Zhou, (2014b). Bioactive coating with hierarchical double porous structure on titanium surface formed by two-step microarc oxidation treatment. *Surface and Coatings Technology*, *252*, 148-156.

R.O. Hussein, D.O. Northwood, X. Nie, (2012). The influence of pulse timing and current mode on the microstructure and corrosion behaviour of a plasma electrolytic oxidation (PEO) coated AM60B magnesium alloy. *Journal of Alloys and Compounds*, *541*, 41-48.

R.O. Hussein, X. Nie, D.O. Northwood, A.L. Yerokhin, A. Matthews, (2010). Spectroscopic study of electrolytic plasma and discharging behaviour during the plasma electrolytic oxidation (PEO) process. *Journal of Physics D Applied Physics*, *43*(10), 105203.

S. Abbasi, F. Golestani-Fard, H.R. Rezaie, S.M.M. Mirhosseini, (2012). MAO-derived hydroxyapatite/TiO2 nanostructured multi-layer coatings on titanium substrate. *Applied Surface Science*, *261*, 37-42.

S. Abbasi, F. Golestani-Fard, S.M.M. Mirhosseini, A. Ziaee, M. Mehrjoo, (2013). Effect of electrolyte concentration on microstructure and properties of micro arc oxidized hydroxyapatite/titania nanostructured composite. *Materials Science and Engineering: C*, *33*(5), 2555-2561.

S. Aliasghari, P. Skeldon, G.E. Thompson, (2014). Plasma electrolytic oxidation of titanium in a phosphate/silicate electrolyte and tribological performance of the coatings. *Applied Surface Science, 316*, 463-476.

S. Cheng, D. Wei, Y. Zhou, (2012). The effect of oxidation time on the micro-arc titanium dioxide surface coating containing Si, Ca and Na. *Procedia Engineering*, *27*, 713-717.

S. Durdu, Ö.F. Deniz, I. Kutbay, M. Usta, (2013). Characterization and formation of hydroxyapatite on Ti6Al4V coated by plasma electrolytic oxidation. *Journal of Alloys and Compounds*, 551, 422-429.

S. Eraković, A. Janković, I.Z. Matić, Z.D. Juranić, M. Vukašinović-Sekulić, T. Stevanović, V. Mišković-Stanković, (2013). Investigation of silver impact on hydroxyapatite/lignin coatings electrodeposited on titanium. *Materials Chemistry and Physics*, *142*(2), 521-530.

S. Kim, S.H. Ku, S.Y. Lim, J.H. Kim, C.B. Park, (2011). Graphene-Biomineral Hybrid Materials. *Advanced Materials*, *23*(17), 2009-2014.

S. Lederer, S. Arat, W. Fuerbeth, (2021). Influence of Process Parameters on the Tribological Behavior of PEO Coatings on CP-Titanium 4+ Alloys for Biomedical Applications. *Materials*.

S. Liu, G. Lai, H. Zhang, A. Yu, (2017). Amperometric aptasensing of chloramphenicol at a glassy carbon electrode modified with a nanocomposite consisting of graphene and silver nanoparticles. *Microchimica Acta*, *184*(5) 1-7.

S. Liu, T.H. Zeng, M. Hofmann, E. Burcombe, J. Wei, R. Jiang, J. Kong, Y. Chen, (2011). Antibacterial activity of graphite, graphite oxide, graphene oxide, and reduced graphene oxide: membrane and oxidative stress. *Acs Nano*, *5*(9), 6971-80.

S. Liu, X. Yang, Z. Cui, S. Zhu, Q. Wei, (2011). One-step synthesis of petal-like apatite/titania composite coating on a titanium by micro-arc oxidation. *Materials Letters*, *65*(6), 1041-1044.

S. Sikdar, P.V. Menezes, R. Maccione, T. Jacob, P.L. Menezes, (2021). Plasma Electrolytic Oxidation (PEO) Process — Processing, Properties, and Applications. *Nanomaterials*.

S. Stojadinovic, N. Tadic, N.M. Sisovic, R. Vasilic, (2015). Real-time imaging, spectroscopy, and structural investigation of cathodic plasma electrolytic oxidation of molybdenum. *Journal of Applied Physics*, *117*(23), 66.

S. Wang, X. Wang, F.G. Draenert, O. Albert, H.C. Schröder, V. Mailänder, G. Mitov, W.E.G. Müller, (2014). Bioactive and biodegradable silica biomaterial for bone regeneration. *Bone*, *67*, 292-304.

S. Wang, Y. Xia, L. Liu, N. Si, (2014). Preparation and performance of MAO coatings obtained on AZ91D Mg alloy under unipolar and bipolar modes in a novel dual electrolyte. *Ceramics International*, *40*(1, Part A), 93-99.

S. Xin, L. Song, R. Zhao, X. Hu, (2006). Influence of cathodic current on composition, structure and properties of Al2O3 coatings on aluminum alloy prepared by micro-arc oxidation process. *Thin Solid Films*, *515*(1), 326-332.

S.B. Maddinedi, B.K. Mandal, N.K. Fazlur-Rahman, (2017). High reduction of 4-nitrophenol using reduced graphene oxide/Ag synthesized with tyrosine. *Environmental Chemistry Letters*.

S.H. Ku, M. Lee, C.B. Park, (2013). Carbon-Based Nanomaterials for Tissue Engineering. *Advanced Healthcare Materials*, *2*(2), 244-260.

S.-R. Ryoo, Y.-K. Kim, M.-H. Kim, D.-H. Min, (2010). Behaviors of NIH-3T3 Fibroblasts on Graphene/Carbon Nanotubes: Proliferation, Focal Adhesion, and Gene Transfection Studies. *ACS Nano*, *4*(11), 6587-6598.

S.V. Gnedenkov, O.A. Khrisanfova, A.G. Zavidnaya, S.L. Sinebryukhov, V.S. Egorkin, M.V. Nistratova, A. Yerokhin, A. Matthews, (2010). PEO coatings obtained on an Mg–Mn type alloy under unipolar and bipolar modes in silicate-containing electrolytes. *Surface and Coatings Technology*, *204*(14), 2316-2322.

V. K, R. N, S. D, S. M, B. Ac, M. V, S. S, (2013). Role of electrolyte chemistry on electronic and in vitro electrochemical properties of micro-arc oxidized titania films on Cp Ti. *Electrochimica Acta*, *105*, 468-480.

W. Chen, S. Li, C. Chen, L. Yan, (2011). Self-assembly and embedding of nanoparticles by in situ reduced graphene for preparation of a 3D graphene/nanoparticle aerogel. *Advanced Materials*, *23*(47), 5679-5683.

W. Hu, C. Peng, W. Luo, M. Lv, X. Li, D. Li, Q. Huang, C. Fan, (2010). Graphene-based antibacterial paper. *Acs Nano*, *4*(7), 4317-4323.

W. Simka, (2019). Anodization of a Medical-Grade Ti-6Al-7Nb Alloy in a Ca(H2PO2)2-Hydroxyapatite Suspension. *Materials*, 12.

W. Simka, R.P. Socha, G. Dercz, J. Michalska, A. Maciej, A. Krząkała, (2013). Anodic oxidation of Ti–13Nb–13Zr alloy in silicate solutions. *Applied Surface Science*, *279*, 317-323.

W. Zhang, Q. Chang, L. Xu, G. Li, G. Yang, X. Ding, X. Wang, D. Cui, X. Jiang, (2016). Graphene Oxide-Copper Nanocomposite-Coated Porous CaP Scaffold for Vascularized Bone Regeneration via Activation of Hif-1α. *Advanced Healthcare Materials*, *5*(11), 1299-1309.

W. Zhu, Y.-J. Fang, H. Zheng, G. Tan, H. Cheng, C. Ning, (2013). Effect of applied voltage on phase components of composite coatings prepared by micro-arc oxidation. *Thin Solid Films*, *544*, 79-82.

W. Zhu, Z. Zhang, B. Gu, J. Sun, L. Zhu, (2013). Biological Activity and Antibacterial Property of Nano-structured TiO2 Coating Incorporated with Cu Prepared by Micro-arc Oxidation. *Journal of Materials Science & Technology*, *29*(3), 237-244.

W.-C. Gu, G.-H. Lv, H. Chen, G.-L. Chen, W.-R. Feng, G.-L. Zhang, S.-Z. Yang, (2007). Preparation of ceramic coatings on inner surface of steel tubes using a combined technique of hot-dipping and plasma electrolytic oxidation. *Journal of Alloys and Compounds*, *430*(1), 308-312.

W.-H. Song, Y.-K. Jun, Y. Han, S.-H. Hong, (2004). Biomimetic apatite coatings on micro-arc oxidized titania. *Biomaterials*, *25*(17), 3341-3349.

X. Fan, B. Feng, Y. Di, X. Lu, K. Duan, J. Wang, J. Weng, (2012). Preparation of bioactive TiO film on porous titanium by micro-arc oxidation. *Applied Surface Science*, *258*(19), 7584-7588.

X. Lin, L. Tan, Q. Wang, G. Zhang, B. Zhang, K. Yang, (2013). In vivo degradation and tissue compatibility of ZK60 magnesium alloy with micro-arc oxidation coating in a transcortical model. *Materials Science and Engineering: C*, *33*(7), 3881-3888.

X. Shen, Y. Hu, G. Xu, W. Chen, K. Xu, Q. Ran, P. Ma, Y. Zhang, J. Li, K. Cai, (2014). Regulation of the Biological Functions of Osteoblasts and Bone Formation by Zn-Incorporated Coating on Microrough Titanium. *ACS Applied Materials & Interfaces*, *6*(18), 16426-16440.

X. Sun, Z. Jiang, S. Xin, Z. Yao, (2005). Composition and mechanical properties of hard ceramic coating containing α-Al2O3 produced by microarc oxidation on Ti–6Al–4V alloy. *Thin Solid Films*, *471*(1), 194-199.

X. Yao, X. Zhang, H. Wu, L. Tian, Y. Ma, B. Tang, (2014). Microstructure and antibacterial properties of Cu-doped TiO2 coating on titanium by micro-arc oxidation. *Applied Surface Science*, *292*, 944-947.

X. Zhang, J. Li, X. Wang, Y. Wang, R. Hang, X. Huang, B. Tang, P.K. Chu, (2018). Effects of copper nanoparticles in porous TiO2 coatings on bacterial resistance and cytocompatibility of osteoblasts and endothelial cells. *Materials Science and Engineering: C*, *82*, 110-120.

X. Zhang, Z. Yao, Z. Jiang, Y. Zhang, X. Liu, (2011). Investigation of the plasma electrolytic oxidation of Ti6Al4V under single-pulse power supply. *Corrosion Science*, *53*(6), 2253-2262.

Y. Bai, I.S. Park, S.J. Lee, T.S. Bae, W. Duncan, M. Swain, M.H. Lee, (2011). One-step approach for hydroxyapatite-incorporated TiO2 coating on titanium via a combined technique of micro-arc oxidation and electrophoretic deposition. *Applied Surface Science*, *257*(15), 7010-7018.

Y. Chang, S.-T. Yang, J.-H. Liu, E. Dong, Y. Wang, A. Cao, Y. Liu, H. Wang, (2011). In vitro toxicity evaluation of graphene oxide on A549 cells. *Toxicology Letters*, *200*(3), 201-210.

Y. Ma, H. Di, Z. Yu, L. Liang, L. Lv, Y. Pan, Y. Zhang, D. Yin, (2016). Fabrication of silica-decorated graphene oxide nanohybrids and the properties of composite epoxy coatings research. *Applied Surface Science*, *360*(jan.1pt.B), 936-945.

Y. Qiao, W. Zhang, P. Tian, F. Meng, H. Zhu, X. Jiang, X. Liu, P.K. Chu, (2014). Stimulation of bone growth following zinc incorporation into biomaterials. *Biomaterials*, *35*(25), 6882-6897.

Y. Tu, M. Lv, P. Xiu, T. Huynh, R. Zhou, (2013). Erratum: Destructive extraction of phospholipids from Escherichia coli membranes by graphene nanosheets (Nature Nanotechnology 8 (594-601)). *Nature Nanotechnology*, *8*(12).

Y. Wang, B. Jiang, T. Lei, L. Guo, (2004). Dependence of growth features of microarc oxidation coatings of titanium alloy on control modes of alternate pulse. *Materials Letters*, *58*(12), 1907-1911.

Y. Wang, H. Yu, C. Chen, Z. Zhao, (2015). Review of the biocompatibility of micro-arc oxidation coated titanium alloys. *Materials & Design*, *85*, 640-652.

Y. Yangi, H. Wu, (2012). Effects of Current Density on Microstructure of Titania Coatings by Micro-arc Oxidation. *Journal of Materials Science & Technology*, *28*(4), 321-324.

Y. Zeng, X. Pei, S. Yang, H. Qin, H. Cai, S. Hu, L. Sui, Q. Wan, J. Wang, (2016). Graphene oxide/hydroxyapatite composite coatings fabricated by electrochemical deposition. *Surface and Coatings Technology*, *286*, 72-79.

Y. Zheng, A. Wang, Z. Wang, L. Fu, F. Peng, (2017). Facial Synthesis of Carrageenan/Reduced Graphene Oxide/Ag Composite as Efficient SERS Platform. *Mat Res*, *20*(ahead).

Y.Y. Shi, M. Li, Q. Liu, Z.J. Jia, Y.F. Zheng, (2016). Electrophoretic deposition of graphene oxide reinforced chitosan–hydroxyapatite nanocomposite coatings on Ti substrate. *J Mater Sci Mater Med*, *27*(3), 48.